

## A Pharmacokinetic Model to Predict the PK Interaction of L-Dopa and Benserazide in Rats

Susan Grange,<sup>1,3</sup> Nicholas H. G. Holford,<sup>2</sup> and Theodor W. Guentert<sup>1</sup>

Received March 13, 2001; accepted May 4, 2001

**Purpose.** To study the PK interaction of L-dopa/benserazide in rats. **Methods.** Male rats received a single oral dose of 80 mg/kg L-dopa or 20 mg/kg benserazide or 80/20 mg/kg L-dopa/benserazide. Based on plasma concentrations the kinetics of L-dopa, 3-O-methyldopa (3-OMD), benserazide, and its metabolite Ro 04-5127 were characterized by noncompartmental analysis and a compartmental model where total L-dopa clearance was the sum of the clearances mediated by amino-acid-decarboxylase (AADC), catechol-O-methyltransferase and other enzymes. In the model Ro 04-5127 inhibited competitively the L-dopa clearance by AADC.

**Results.** The coadministration of L-dopa/benserazide resulted in a major increase in systemic exposure to L-dopa and 3-OMD and a decrease in L-dopa clearance. The compartmental model allowed an adequate description of the observed L-dopa and 3-OMD concentrations in the absence and presence of benserazide. It had an advantage over noncompartmental analysis because it could describe the temporal change of inhibition and recovery of AADC.

**Conclusions.** Our study is the first investigation where the kinetics of benserazide and Ro 04-5127 have been described by a compartmental model. The L-dopa/benserazide model allowed a mechanism-based view of the L-dopa/benserazide interaction and supports the hypothesis that Ro 04-5127 is the primary active metabolite of benserazide.

**KEY WORDS:** L-dopa; 3-O-methyldopa; benserazide; PK drug-drug interaction; amino acid decarboxylase.

### INTRODUCTION

L-Dopa (L-3,4-dihydroxyphenylalanine), a dopamine precursor, is used for the treatment of Parkinsonism, which occurs due to a deficiency of dopamine neurotransmission in the striatum (1). Dopamine itself is not suitable for treatment because it does not cross the blood-brain barrier and it is not active orally as a result of enzymatic degradation in the gut and first-pass metabolism (2). In contrast to dopamine, L-dopa enters the brain and is decarboxylated to dopamine. L-dopa is well absorbed, but rapidly and extensively metabolized in the periphery, predominantly in the gut and the liver. The decarboxylation of L-dopa to dopamine by amino acid decarboxylase (AADC) is a major biotransformation pathway (69%) for L-dopa (3). A second, but less important pathway (10%) is the O-methylation of L-dopa to 3-O-methyldopa (3-OMD) by catechol-O-methyltransferase (COMT) (3). Peripheral dopamine formation causes side effects (neu-

sea and cardiac arrhythmias) (4). Therefore, L-dopa is given together with a peripheral AADC inhibitor such as benserazide or carbidopa. Benserazide (seryl-trihydroxybenzylhydrazine) is mainly metabolized in the gut to its active metabolite Ro 04-5127 (trihydroxybenzylhydrazine).

The pharmacokinetics of L-dopa in rats after administration of L-dopa alone or L-dopa combined with a peripheral AADC inhibitor has been studied mainly using noncompartmental analysis (see, e.g., 5–8). Compartmental modelling was used infrequently to describe L-dopa disposition in non-humans (5,9–11). No attempt has been made to model the inhibition of L-dopa decarboxylation after benserazide administration and its effect on the kinetics of L-dopa and its metabolite 3-OMD in a mechanistic way. The objective of our investigation was to develop a model for the PK interaction of L-dopa and benserazide in rats to better understand the use of these drugs in humans.

### MATERIALS AND METHODS

#### Drugs and Chemicals

All chemicals used were of analytical grade. L-Dopa and benserazide were provided by F. Hoffmann-La Roche Ltd. For administration L-dopa and benserazide were separately dissolved in 0.9% NaCl (L-dopa 20 mg/ml, benserazide 10 mg/ml).

#### Animal Experiment

Twenty-one male albino rats (strain: Wistar/Füllinsdorf) weighing 262–307 g and 3 male albino rats (strain: RoRo/Füllinsdorf) weighing 309–323 g were used in this study. The age of the rats was 10–12 weeks. A single dose, parallel design with three treatments, 20 mg/kg (78  $\mu$ mol/kg) benserazide po or 80 mg/kg (406  $\mu$ mol/kg) L-dopa po or 80 mg/kg L-dopa + 20 mg/kg benserazide, was employed. Six rats (strain: Wistar/Füllinsdorf) were assigned to each treatment group. Another 3 rats (same strain) were included in the experiment for collecting predose samples. They did not receive any treatment. In the treatment group where 80/20 mg/kg L-dopa/benserazide was given, an additional 3 rats (strain: RoRo/Füllinsdorf) were studied. These were also Wistar rats, which were bred at F. Hoffmann-La Roche Ltd. They were studied additionally to compare the present data with former company studies where only RoRo rats had been used. A catheter was implanted in the jugular vein for blood sampling 2 days before drug administration. Blood was collected for the determination of L-dopa, 3-OMD, benserazide, and Ro 04-5127. The blood sampling schedules were 0, 0.083, 0.17, 0.25, 0.5, 1, 2, 3, and 4 h after benserazide treatment and 0, 0.083, 0.17, 0.25, 0.5, 1, 2, 3, 4, 6, 8, 10, and 24 h after L-dopa treatment and L-dopa/benserazide treatment. All samples were stabilized by adding sodium metabisulfite immediately after blood collection (5 mg/ml blood) and a second time to each plasma sample (5 mg/ml plasma) immediately after centrifugation. The blood samples were centrifuged at 3500  $\times$  g for 5 min and the plasma samples were kept at  $-80^{\circ}\text{C}$  until analysis. The samples containing benserazide and Ro 04-5127 were ana-

<sup>1</sup> PRNS Non-Clinical Drug Safety, F. Hoffmann-La Roche Ltd., 4070 Basel, Switzerland.

<sup>2</sup> Division Pharmacology and Clinical Pharmacology, University of Auckland, Private Bag 92019, Auckland, New Zealand.

<sup>3</sup> To whom correspondence should be addressed. (e-mail: susan.grange@roche.com)

lyzed within 8 days, taking the compound's known instability into account (12). This study was carried out in accordance with Art. 62 of the Swiss Federal Ordinance on the Protection of Animals.

### Analytical Assay

Two separate analytical methods were used to determine plasma concentrations of L-dopa and its metabolite 3-OMD and benserazide and its metabolite Ro 04-5127, both using HPLC-electrochemical detection methodologies (13,14). The analytes together with internal standards (alpha-ethyl-dopa for L-dopa/3-OMD, a methylated derivative of benserazide for benserazide/Ro 04-5127) were isolated from plasma by solid phase extraction using cation exchange cartridges (1 ml/100 mg SCX, Bondelut, Varian) in the L-dopa/3-OMD assay and aluminum oxide cartridges (1 ml/100 mg Alox-A, Bondelut, Varian) in the benserazide/Ro 04-5127 assay. Gradient elution and ion pair formation of the cationic compounds with anionic-pairing reagent at acidic pH was performed to separate the analytes from residual plasma constituents. A phosphate buffer (100 nM)/acetonitrile gradient containing 5 mM 1-octanesulfonic acid and 0.5 mM EDTA was used as mobile phase. The analytes were quantified with amperometric detection.

The concentrations of the analytes were determined using a calibration curve calculated by linear least squares regression of peak height ratios (peak height of analyte/peak height of internal standard) vs. nominal concentration using standard operating procedures. New curves were prepared with each batch of analytical samples. The calibration samples were prepared from human plasma (dialyzed for the L-dopa/3-OMD assay) and stabilized with 10 mg/ml sodium metabisulfite. The calibration range in this study was generally 1–500 µg/l (L-dopa, 3-OMD) and 0.25–50 µg/l (benserazide, Ro 04-5127).

The quantification limits were determined by analyzing spiked plasma samples repeatedly over 5 days around the expected determination limit. The quantification limits for this study were defined as 0.85 µg/l (L-dopa, 3-OMD) and 0.20 µg/l (benserazide, Ro 04-5127) (inter-assay precision ≤20%; inaccuracy ≤15%). Quality control samples at different appropriate concentrations were prepared and analyzed in duplicate with each assay batch (approx. 18–43% quality control samples referenced to the number of unknown samples). Results from unknown samples were accepted only if less than 25% of the quality control samples within each assay batch had an inaccuracy greater than 15% (L-dopa, 3-OMD) or 20% (benserazide, Ro 04-5127).

### Pharmacokinetic Analysis

The plasma concentration-time curves of L-dopa, 3-OMD, benserazide, and Ro 04-5127 were analyzed by non-compartmental methods and by applying a compartmental model to the data to describe the PK interaction of L-dopa and benserazide. Visual inspection of the concentration-time profiles did not reveal any difference between the strains (Wistar, RoRo). To increase the data density for the modeling process the data of the RoRo rats were included.

The maximum plasma concentrations after a dose ( $C_{max}$ ) and the times of their occurrence ( $T_{max}$ ) were determined directly from the observed data. The beginning of the terminal log-linear phase was estimated by eye from log-linear plots and its slope, reflecting the terminal rate constant ( $k$ ), calculated by log-linear regression analysis. The terminal half-life ( $T_{1/2}$ ) was derived from  $\ln(2)/k$ . The absorption rate constant ( $k_a$ ) was estimated by the method of residuals (15). The areas under plasma concentration vs. time curves from time zero to infinity ( $AUC_{0-\infty}$ ) were obtained by applying the linear trapezoidal rule up to  $C_{max}$  and the logarithmic trapezoidal rule after  $C_{max}$  up to the last observed concentration using actual sampling times. Extrapolation to time infinity ( $\hat{C}_{last}/k$ ) was achieved using predicted concentrations at the last observation time point ( $\hat{C}_{last}$ ), which were calculated from the regression line (16). The oral clearance (CL/F) after a single oral dose was calculated by dose/ $AUC_{0-\infty}$ . Dividing CL/F by  $k$  gave an estimate of the volume of distribution (V/F).

For the compartmental analysis the kinetics of L-dopa and 3-OMD after 80 mg/kg L-dopa and 80/20 mg/kg L-dopa/benserazide were described by a 1-compartment model (first-order absorption) where total L-dopa clearance ( $CL_{dopa}$ ) was the sum of the clearances mediated by AADC, COMT and other elimination pathways (Eq. 1).

$$CL_{dopa} = CL_{AADC} + CL_{COMT} + CL_{REST} \quad (1)$$

If L-dopa was administered alone the model was set up such that 69% (3) of L-dopa were metabolized by AADC ( $f_{AADC}$ ), 10% (3) by COMT ( $f_{COMT}$ ) and the rest, 21%, by other enzymes. After administration of L-dopa together with benserazide those metabolic fractions were allowed to change in relation to the extent of inhibition. Ro 04-5127 was assumed to inhibit competitively (17) the L-dopa clearance mediated by AADC ( $CL_{AADC}$ ) and thereby to affect the total L-dopa clearance and the availability of L-dopa from the gut and across the liver.  $CL_{AADC}$  was estimated by Eq. 2 where  $CL_{AADC0}$  was the L-dopa clearance via AADC with no inhibition,  $C_{1M}$  was the Ro 04-5127 concentration (inhibitor concentration) and  $k_i$  was the inhibition constant.

$$CL_{AADC} = \frac{CL_{AADC0}}{\left(1 + \frac{C_{1M}}{k_i}\right)} \quad (2)$$

Therefore, the total L-dopa clearance varied after L-dopa/benserazide due to the change in  $CL_{AADC}$  caused by the inhibitor, whereas the total L-dopa clearance after L-dopa was a constant value which was estimated as a primary parameter in the model.

The hepatic availability ( $F_H$ ) was described by Eq. 3 where the ratio of hepatic blood clearance of L-dopa ( $CL_H$ ) to hepatic blood flow ( $Q$ ; 0.828 l/h/0.25 kg (18)) was subtracted from 1. The hepatic blood clearance of L-dopa was obtained from the product of the hepatically cleared fraction ( $f_H$ ) and the total blood clearance of L-dopa (Eq. 4). Because the blood/plasma ratio of L-dopa was approximately 1.0 (19) the total plasma clearance of L-dopa, a primary parameter in the model, was set equal to the total blood clearance of L-dopa. The majority of L-dopa is metabolized extrahepatically.

cally and the hepatic clearance of L-dopa was assumed to be 13% of total body clearance (19).

$$F_H = 1 - \frac{CL_H}{Q} \quad (3)$$

$$CL_H = f_H \times CL_{\text{dopa}} \quad (4)$$

The gastrointestinal availability ( $F_G$ ) was obtained from the literature (0.244 (11)) after administration of L-dopa and was set to 1 after administration of L-dopa/benserazide. The overall oral bioavailability of L-dopa ( $F$ ) was estimated by  $F_G \cdot F_H$ . A distinction was made between absorption parameters after L-dopa ( $ka_b$ ,  $F_b$ ) and absorption parameters after L-dopa/benserazide ( $ka_c$ ,  $F_c$ ). Based on initial modelling results the 3-OMD parameters, clearance and volume of distribution, were subsequently allowed to differ between the treatments L-dopa and L-dopa/benserazide ( $CL_{\text{OMD},b}$ ,  $CL_{\text{OMD},c}$ ,  $V_{\text{OMD},b}$ ,  $V_{\text{OMD},c}$ ). The mass balances for the compartments of L-dopa and 3-OMD were described by differential equations (Eq. 5 to Eq. 7).

$$\frac{dA_{\text{dopa},i}}{dt} = -ka_i \times A_{\text{dopa},i}(t) \quad (5)$$

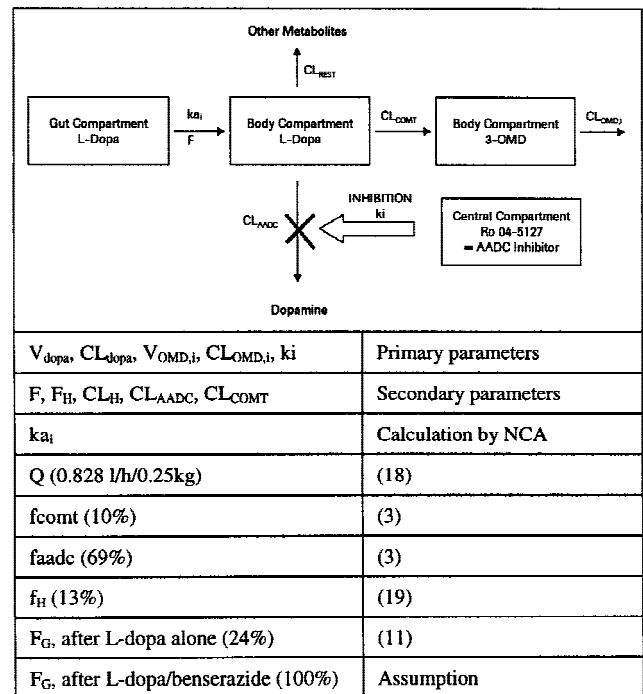
$$V_{\text{dopa}} \times \frac{dC_{\text{dopa},i}}{dt} = ka_i \times A_{\text{dopa},i}(t) \times F_i - CL_{\text{dopa}} \times C_{\text{dopa},i}(t) \quad (6)$$

$$V_{\text{OMD},i} \times \frac{dC_{\text{OMD},i}}{dt} = CL_{\text{COMT}} \times C_{\text{dopa},i}(t) - CL_{\text{OMD},i} \times C_{\text{OMD},i}(t) \quad (7)$$

where  $A_{\text{dopa},i}$  = amount L-dopa in gut compartment,  $C_{\text{dopa},i}$  = L-dopa concentration in systemic compartment,  $C_{\text{OMD},i}$  = 3-OMD concentration in systemic compartment,  $i = b$  (treatment L-dopa); and  $i = c$  (treatment L-dopa/benserazide).

The kinetics of benserazide and its metabolite Ro 04-5127 were described with 2-compartment models. After oral administration of benserazide the amount of Ro 04-5127 in plasma was assumed to be derived from the sum of metabolite formed systemically and presystemically. To model the kinetics of the metabolite Ro 04-5127 three further assumptions were necessary. The elimination of Ro 04-5127 was assumed to be the fastest process of all the first-order processes governing the kinetics of Ro 04-5127. Therefore, a rough approximation of the elimination rate constant ( $ke_M$ ) was obtained from  $\ln(2)/(T_{\text{max}}/3)$ . The fraction of Ro 04-5127 absorbed from the gut was assumed to be 7%. The fraction of benserazide metabolized to Ro-04-5127 systemically,  $f_m$ , was assumed to be 15%.

Figures 1 and 2 show the schematic diagram of the conceptual model for L-dopa and benserazide. The data pooled per analyte was analyzed using the naive pooled data approach. In a first step the L-dopa model was fitted simultaneously to the L-dopa and 3-OMD data after treatment with 80 mg/kg L-dopa. In a second step the model including inhibition of the AADC pathway was fitted simultaneously to the L-dopa and 3-OMD data after treatment with 80/20 mg/kg L-dopa/benserazide. Those parameters, which could be estimated in the first step, were fixed in the second step. The estimated primary parameters were the volume of distribution of L-dopa ( $V_{\text{dopa}}$ ), the total clearance of L-dopa ( $CL_{\text{dopa}}$ )



$i = b$  (treatment L-dopa);  $i = c$  (treatment L-dopa/benserazide)

**Fig. 1.** Schematic diagram of conceptual model to describe kinetics of L-dopa and 3-OMD ( $Q$  hepatic blood flow, L-dopa:  $CL_{\text{AADC}}$  clearance via AADC,  $CL_{\text{AADC}0}$  clearance via AADC (no inhibition),  $CL_{\text{COMT}}$  clearance via COMT,  $CL_{\text{dopa}}$  total clearance,  $CL_H$  hepatic clearance,  $CL_{\text{REST}}$  clearance via other elimination pathways,  $f_{\text{AACD}}$  fraction metabolized by AADC,  $f_{\text{COMT}}$  fraction metabolized by COMT,  $f_H$  hepatic fraction of total L-dopa clearance,  $V_{\text{dopa}}$  volume of distribution,  $F$  bioavailability ( $F_G \cdot F_H$ ),  $F_H$  hepatic availability,  $F_G$  gastrointestinal availability,  $ka_i$  absorption rate constant; 3-OMD:  $CL_{\text{OMD},i}$  clearance,  $V_{\text{OMD},i}$  volume of distribution; Ro 04-5127:  $ki$  inhibition constant).

after L-dopa, the volume of distribution of 3-OMD after L-dopa ( $V_{\text{OMD},b}$ ) and after L-dopa/benserazide ( $V_{\text{OMD},c}$ ), the 3-OMD clearance after L-dopa ( $CL_{\text{OMD},b}$ ) and after L-dopa/benserazide ( $CL_{\text{OMD},c}$ ), and the inhibition constant ( $ki$ ). The secondary parameters after treatment with L-dopa were the bioavailability of L-dopa ( $F$ ), the hepatic availability of L-dopa ( $F_H$ ), the hepatic clearance of L-dopa ( $CL_H$ ), the L-dopa clearance by AADC, and the L-dopa clearance by COMT. The constants of the model were the L-dopa dose, the absorption rate constant of L-dopa after L-dopa ( $ka_b$ ) and after L-dopa/benserazide ( $ka_c$ ), the hepatic blood flow, the L-dopa fraction metabolized by COMT after L-dopa ( $f_{\text{comt}}$ ), the L-dopa fraction metabolized by AADC after L-dopa ( $f_{\text{aacd}}$ ), the hepatic fraction of L-dopa ( $f_H$ ), and the gastrointestinal availability of L-dopa after L-dopa and after L-dopa/benserazide. The benserazide/Ro 04-5127 data were fitted separately and the estimated parameters for the benserazide/Ro 04-5127 kinetics were used as fixed parameters in the L-dopa model.

The benserazide/Ro 04-5127 model was fitted simultaneously to the oral data of benserazide and Ro 04-5127 (pooled data from both treatments including benserazide) of the present study as well as intravenous data of benserazide and Ro 04-5127 from two previous studies (20,21) (see below). The estimated primary parameters in the benserazide

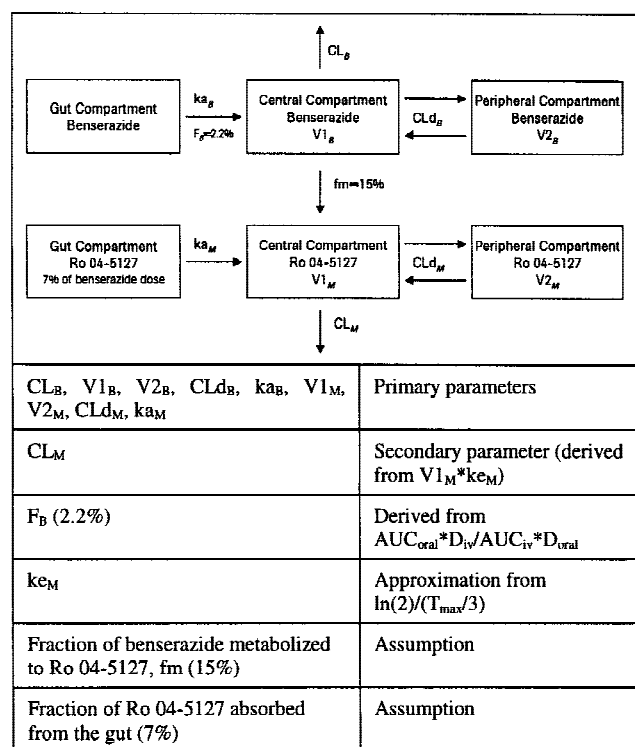


**Fig. 2.** Schematic diagram of conceptual model to describe kinetics of benserazide and Ro 04-5127 (benserazide:  $CL_B$  total clearance,  $CL_{dB}$  intercompartmental clearance,  $F_B$  bioavailability,  $f_m$  fraction metabolized,  $k_{aB}$  absorption rate constant,  $V_{1B}$  volume of central compartment,  $V_{2B}$  volume of peripheral compartment; Ro 04-5127:  $CL_M$  total clearance,  $CL_{dM}$  intercompartmental clearance,  $k_{aM}$  absorption rate constant,  $ke_M$  elimination rate constant,  $V_{1M}$  volume of central compartment,  $V_{2M}$  volume of peripheral compartment).

model were the volumes of the central compartment ( $V_{1B}$ ,  $V_{1M}$ ) the volumes of the peripheral compartment ( $V_{2B}$ ,  $V_{2M}$ ), the intercompartmental clearances ( $CL_{dB}$ ,  $CL_{dM}$ ), and the absorption rate constants ( $k_{aB}$ ,  $k_{aM}$ ). The clearance for benserazide ( $CL_B$ ) was a further primary parameter while for Ro 04-5127 it was derived from  $V_{1M} \cdot ke_M$  ( $CL_M$ ). The constants in the benserazide model were the benserazide dose, the bioavailability of benserazide, the fraction of Ro 04-5127 absorbed from the gut, the fraction of benserazide metabolized to Ro 04-5127, and the elimination rate constant of Ro 04-5127 ( $ke_M$ ).

The weighting was selected empirically by judging the goodness of fit. In the L-dopa model it was  $1/Y^{0.25}$  for both steps. The weighting was  $1/Y^2$  after intravenous administration of benserazide. Unit weighting was applied to model the data after oral administration of benserazide.

The integration algorithm was 4th–5th order Runge-Kutta with variable step size. The parameters were evaluated by nonlinear least squares estimation, using the simplex algorithm for minimizing the sum of squared residuals. The modelling analysis was performed on a Pentium Pro 200 Mhz (RAM 96 MB, HD 2 GB; Windows NT 4.0 SP3) computer using WinNonlin 1.5 (Pharsight Corporation).

### Statistical Analysis

An unpaired Student's *t* test was used to compare the log-transformed (22) parameters of L-dopa or 3-OMD be-

tween treatment L-dopa and treatment L-dopa/benserazide and to compare the log-transformed (22) parameters of benserazide or Ro 04-5127 between treatment benserazide and treatment L-dopa/benserazide. The level of statistical significance was defined as  $p < 0.05$ . If no statistically significant difference was found between treatments a 95% confidence interval for the true mean ratio (95% CI) was calculated. The Student's *t* test was not applicable for  $T_{max}$  because it is a discrete variable.

### Intravenous Data of Benserazide and Ro 04-5127

In the benserazide/Ro 04-5127 model intravenous data was incorporated from two previous studies (20,21). The data were obtained from 5 male rats (strain: RoRo/Füllinsdorf) that received 5 mg/kg (19  $\mu$ mol/kg) benserazide intravenously.

## RESULTS

### Animal Experiment

Rat a4 of treatment group 20 mg/kg benserazide and rat b6 of treatment group 80 mg/kg L-dopa died before dosing due to problems with the jugular vein catheter. They were not replaced.

### Noncompartmental PK Analysis of L-Dopa and 3-OMD

The 24-h sampling period was sufficient in all instances to describe the concentration-time curve of L-dopa and 3-OMD and to allow a reliable estimation of the terminal half-life and  $AUC_{0-\infty}$ . The L-dopa kinetics of one rat after treatment with L-dopa did not follow a monophasic decline as in the other rats, but showed a biphasic decline. Therefore, its terminal half-life was not included in the statistical evaluation. The 24-h L-dopa values of three rats after treatment with L-dopa/benserazide were around the limit of quantification. They were not used for the estimation of the terminal rate constant. The absorption of L-dopa started rapidly in all rats, leading to a maximum concentration of L-dopa within 1 h after L-dopa dosing. The formation of the metabolite 3-OMD reached a maximum concentration within 4 h after L-dopa administration and within 6 h after L-dopa/benserazide administration. Average concentrations of L-dopa and 3-OMD at various time points after L-dopa dosing of each treatment are shown in Fig. 3. The average values of L-dopa and 3-OMD parameters are listed in Table I and Table II. The L-dopa and 3-OMD kinetics were different with and without benserazide. A statistically significant difference ( $*p < 0.01$ ,  $**p < 0.05$ ) was found for the L-dopa parameters  $AUC_{0-\infty}^*$ ,  $C_{max}^*$ ,  $CL/F^*$ ,  $T_{1/2}^*$ , and  $ka^{**}$  and for the 3-OMD parameters  $AUC_{0-\infty}^*$ ,  $C_{max}^*$ , and  $T_{1/2}^*$ . The co-administration of 80/20 mg/kg L-dopa/benserazide resulted in an 11-fold increase in the L-dopa  $AUC_{0-\infty}$  and a 6-fold increase in  $C_{max}$  of L-dopa. The oral clearance of L-dopa was 9-fold lower after treatment with L-dopa/benserazide than after L-dopa. The half-life of L-dopa was longer by a factor 2 after L-dopa/benserazide treatment. There was a small difference in  $T_{max}$  between the two treatment groups. However, in both cases the between-animal variability of  $T_{max}$  was high. The absorption rate constant was higher after L-dopa than after L-dopa/benserazide. The effect of benserazide on the 3-OMD kinetics was a 15-

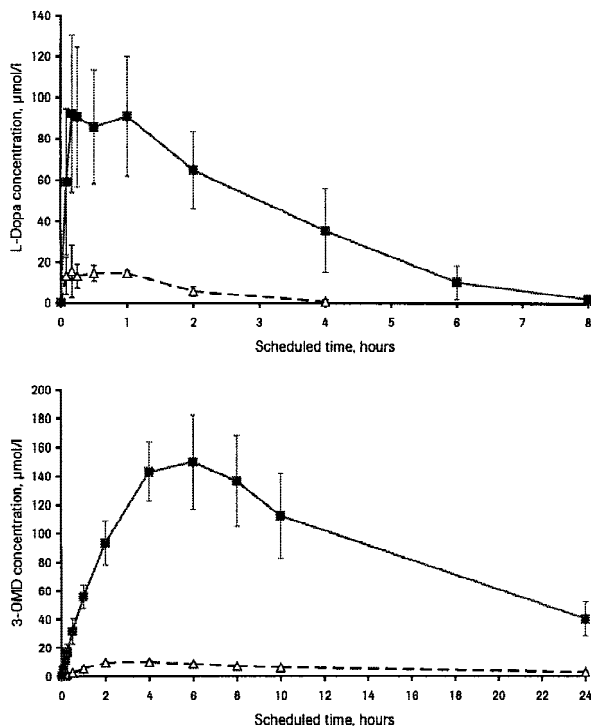


**Fig. 3.** Average ( $\pm$ SD) plasma concentration-time profiles of L-dopa and 3-OMD after treatment with L-dopa ( $-\Delta-$ ) and after treatment with L-dopa/benserazide ( $-\blacksquare-$ ).

fold increase in  $AUC_{0-\infty}$  and  $C_{max}$  of 3-OMD. The half-life of 3-OMD was shorter after treatment with L-dopa/benserazide than after L-dopa. There was a small increase in 3-OMD  $T_{max}$  when L-dopa was given together with benserazide. The oral clearance of 3-OMD after 80 mg/kg L-dopa was  $0.0563 \pm 0.00556$  l/h and the volume of distribution (V/F) was  $0.945 \pm 0.0759$  l. The between-animal variability for the L-dopa parameters  $AUC_{0-\infty}$ ,  $k_a$ ,  $k$ ,  $T_{1/2}$ , CL/F, and V/F was small after treatment with L-dopa. After combined treatment with

**Table I.** Kinetic Parameters<sup>a</sup> of L-Dopa After Treatment with L-Dopa or L-Dopa/Benserazide (Noncompartmental Analysis)

		L-Dopa	L-Dopa/Benserazide
$AUC_{0-\infty}$	Mean (CV%)	27.9 (13%)	307 (27%)
[h · $\mu$ mol/l]	Min-Max	22.1–31.2	216–482
$C_{max}$	Mean (CV%)	20.6 (53%)	115 (27%)
[ $\mu$ mol/l]	Min-Max	13.2–38.8	67.4–152
$T_{max}$	Median	1.00	0.50
[h]	Min-Max	0.08–1.00	0.17–1.00
$k_a$	Mean (CV%)	2.11 (22%)	1.29 (60%)
[h <sup>-1</sup> ]	Min-Max	1.56–2.77	0.55–3.25
$k$	Mean (CV%)	1.73 (7%)	0.887 (20%)
[h <sup>-1</sup> ]	Min-Max	1.60–1.90	0.470–1.07
$T_{1/2}$	Mean (CV%)	0.403 (7%)	0.824 (30%)
[h]	Min-Max	0.365–0.433	0.648–1.48
CL/F	Mean (CV%)	3.72 (14%)	0.397 (20%)
[l/h]	Min-Max	3.20–4.59	0.291–0.519
V/F	Mean (CV%)	2.22 (7%)	0.480 (43%)
[l]	Min-Max	2.07–2.42	0.301–0.952
$n$	—	5 <sup>b</sup>	9

<sup>a</sup> Parameters for whole rats; no weight correction applied.

<sup>b</sup>  $n = 4$  (for  $k$ ,  $T_{1/2}$  and V/F).

**Table II.** Kinetic Parameters<sup>a</sup> of 3-OMD After Treatment with L-Dopa or L-Dopa/Benserazide (Noncompartmental Analysis)

		L-Dopa	L-Dopa/Benserazide
$AUC_{0-\infty}$	Mean (CV%)	183 (12%)	2716 (24%)
[h · $\mu$ mol/l]	Min-Max	161–217	1670–3550
$C_{max}$	Mean (CV%)	10.1 (6%)	154 (19%)
[ $\mu$ mol/l]	Min-Max	9.11–10.6	117–186
$T_{max}$	Median	4.03	6.00
[h]	Min-Max	2.05–4.08	4.00–6.00
$k$	Mean (CV%)	0.0602 (17%)	0.0748 (9%)
[h <sup>-1</sup> ]	Min-Max	0.0496–0.0748	0.0624–0.0877
$T_{1/2}$	Mean (CV%)	11.8 (16%)	9.35 (10%)
[h]	Min-Max	9.26–14.0	7.90–11.1
CL/F <sup>b,c</sup>	Mean (CV%)	0.0563 (10%)	—
[l/h]	Min-Max	0.0479–0.0621	—
V/F <sup>b,c</sup>	Mean (CV%)	0.945 (8%)	—
[l]	Min-Max	0.830–1.01	—
$n$	—	5	9

<sup>a</sup> Parameters for whole rats; no weight correction applied.

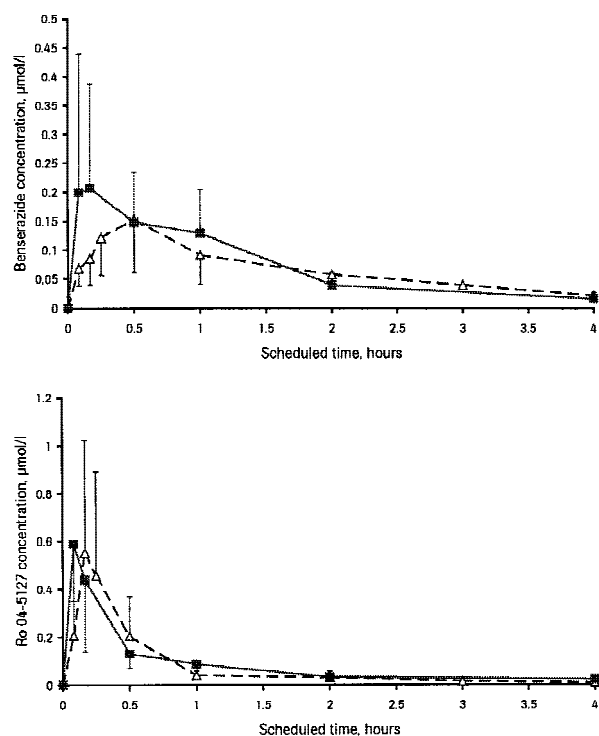
<sup>b</sup> CL/F and V/F were estimated assuming that the fraction metabolized to 3-OMD was 10% (3).

<sup>c</sup> CL/F and V/F cannot be estimated for the L-dopa/benserazide treatment, because the fraction metabolized changes with the degree of inhibition.

L-dopa/benserazide the between-animal variability was several times higher in most cases than after L-dopa.

#### Noncompartmental PK Analysis of Benserazide and Ro 04-5127

The 4-h sampling period was sufficient in all instances to describe the concentration-time curve of benserazide and Ro 04-5127 and to allow a reliable estimation of the terminal half-life and  $AUC_{0-\infty}$ . The absorption of benserazide was fast in all rats, with two exceptions, leading to a maximum benserazide concentration within 0.5 h after benserazide dosing. For two rats  $T_{max}$  was 2 h and 1 h, respectively. The formation of the metabolite Ro 04-5127 reached a maximum concentration of Ro 04-5127 within 0.27 h after benserazide administration and within 0.5 h after L-dopa/benserazide administration. Average concentrations of benserazide and Ro 04-5127 at various time points after benserazide dosing of each treatment are shown in Fig. 4. The average values of benserazide and Ro 04-5127 parameters are listed in Table III and Table IV. The benserazide kinetics were similar with and without L-dopa. No statistically significant difference ( $p < 0.05$ ) was found for  $AUC_{0-\infty}$  (and hence for CL/F),  $C_{max}$ , and V/F between the treatments benserazide and L-dopa/benserazide. The observed mean ratio [(L-dopa with benserazide)/benserazide] for those parameters is presented together with the 95% CI in Table III. After L-dopa/benserazide the maximum plasma benserazide concentration of one rat was about five times higher than the other  $C_{max}$  values. This caused the high variability of  $C_{max}$  in the treatment group L-dopa/benserazide and an upward shift of the average value. The median of  $C_{max}$  and the median of  $AUC_{0-\infty}$  were similar in both treatment groups confirming that the observed upward shift of the average value was due to an individual extreme value. There was no relevant difference in  $T_{1/2}$  and  $k$  between the two treatment groups. After treatment with



<sup>1</sup> The 4h value after treatment with benserazide was the average of two points only.

**Fig. 4.** Average ( $\pm$ SD) plasma concentration-time profiles of benserazide and Ro 04-5127 after treatment with benserazide<sup>1</sup> ( $\Delta$ -) and after treatment with L-dopa/benserazide ( $\blacksquare$ -).

L-dopa/benserazide  $T_{max}$  was smaller than after benserazide. However, the between-animal variability was very high in both groups. The kinetics of Ro 04-5127 were similar with and without L-dopa. No statistically significant difference ( $p < 0.05$ ) was found for  $AUC_{0-\infty}$ ,  $C_{max}$ ,  $T_{1/2}$ , and  $k$  between the treatments benserazide and L-dopa/benserazide. The observed mean ratio [(L-dopa with benserazide)/benserazide] for those parameters is listed together with the 95% CI in Table IV.  $T_{max}$  was similar between the two groups. However, the between-animal variability was high, especially after treatment with L-dopa/benserazide (CV 88%).

#### Compartmental PK Analysis of L-Dopa and 3-OMD

The final parameter estimates of L-dopa and 3-OMD are listed in Table V. After administration of L-dopa the hepatic availability of L-dopa was 87%. Together with the literature value of the gastrointestinal availability of L-dopa ( $F_G$ : 24% (11)) this gave a bioavailability for L-dopa of 21%. Further secondary parameters were the hepatic clearance of L-dopa ( $CL_H$ : 0.107 l/h), the L-dopa clearance by COMT ( $CL_{COMT}$ : 0.0823 l/h), and the L-dopa clearance by AADC ( $CL_{AADC}$ : 0.568 l/h). After administration of L-dopa together with benserazide the availability and clearance terms of L-dopa changed over time dependent on the time course of inhibitor Ro 04-5127. Figure 5 shows the plasma concentration-time profile of Ro 04-5127 and the temporal change of the L-dopa clearance by AADC after L-dopa/benserazide administration. The model fits to combined data sets of treatment with L-dopa and L-dopa/benserazide described the observed concentrations well (Figs. 6 and 7).

#### Compartmental PK Analysis of Benserazide and Ro 04-5127

The final parameter estimates of benserazide and Ro 04-5127 are listed in Table V. The fits to combined data sets of oral and intravenous data described the observed concentrations of benserazide and Ro 04-5127 well.

#### DISCUSSION

The mechanistic models formulated allowed us to adequately describe the observed L-dopa and 3-OMD concentrations in the absence and presence of benserazide. The adequacy of the model was corroborated by the fact that the parameter estimates of L-dopa and 3-OMD of the compartmental analysis were similar to values obtained by noncompartmental analysis (Table VI). Furthermore, the model parameters were also in good agreement with values reported in the literature where available. The L-dopa volume of distribution and the L-dopa clearance of the present study expressed in units per kg body-weight were  $V_{dopa}$  (1.98 l/kg) and  $CL_{dopa}$  (3.29 l/h/kg). Sato *et al.* (10) estimated a volume of distribution ( $V_{d\beta}$ ) of 1.79 l/kg and a clearance of 3.13 l/h/kg for L-dopa. Further L-dopa clearances reported in the literature were 4.46 l/h/kg (11), 5.15 l/h/kg (11), and 1.48 l/h (19). The bioavailability of L-dopa after L-dopa was estimated in the present study to be 21%. This was in good accordance with work done by Iwamoto *et al.* (11).

In the compartmental model the bioavailability of L-dopa was the product of the gastrointestinal availability and the hepatic availability. The availability across the intestinal wall was introduced in addition to the hepatic availability because the gut wall contributes substantially to the overall first-pass effect of L-dopa (11,23). The gastric and intestinal walls are rich in AADC (24,25). This builds an efficient enzymatic barrier for the absorption of L-dopa. Although the liver also has high concentrations of AADC and quickly metabolizes L-dopa (26), it seems to be a less important site of decarboxylation than the gut wall. Peripheral and hepatoportal vein injections of L-dopa gave similar plasma concentrations (19,25,27). In addition, hepatectomy did not create major changes in the disposition of injected L-dopa (28). In the present study the gastrointestinal availability was 24% and the hepatic availability was 87% after oral administration of L-dopa confirming that the gut is the major site of metabolism for L-dopa. After oral administration of L-dopa/benserazide the gastrointestinal availability was assumed to be 100% while the hepatic availability changed dependent on the inhibition ( $F_H \geq 87\%$ ).

The different magnitude of changes in L-dopa's oral clearance (9 fold) and half-life (2-fold) when the drug was given together with benserazide indicates that the change in  $CL/F$  is not only due to the decrease in systemic clearance of L-dopa when combined with benserazide, but also due to a change in the bioavailability of L-dopa. The fact that benserazide has a major effect on the bioavailability is also reflected in the almost 5-fold change in  $V/F$  between treatments. Benserazide affects gut wall AADC controlling the fraction absorbed while changes in systemic L-dopa clearance will be largely due to inhibition of AADC at sites other than the gut wall.

**Table III.** Kinetic Parameters of Benserazide After Treatment with Benserazide or L-Dopa/Benserazide (Noncompartmental Analysis)

		Treatment		Ratio <sup>c</sup> [95% CI]
		Benserazide	L-Dopa/Benserazide	
AUC <sub>0-∞</sub>	Mean (CV%)	0.297 (24%)	0.268 (49%)	0.85 [0.55; 1.32]
[h · μmol/l]	Min-Max	0.224-0.413	0.161-0.569	
C <sub>max</sub>	Mean (CV%)	0.161 (50%)	0.247 (90%)	1.38 [0.70; 2.73]
[μmol/l]	Min-Max	0.0732-0.287	0.123-0.827	
T <sub>max</sub>	Median	0.50	0.17	—
[h]	Min-Max	0.50-2.00	0.10-1.00	
k	Mean (CV%)	0.567 (20%)	0.963 (38%)	—
[h <sup>-1</sup> ]	Min-Max	0.451-0.735	0.400-1.59	
T <sub>1/2</sub>	Mean (CV%)	1.26 (19%)	0.842 (48%)	—
[h]	Min-Max	0.943-1.54	0.436-1.73	
CL/F	Mean (CV%)	70.8 (31%)	95.4 (36%)	1.31 [0.81; 2.12]
[l/h]	Min-Max	48.0-95.1	39.7-144	
V/F	Mean (CV%)	131 (39%)	110 (40%)	[0.82 [0.44; 1.53]
[l]	Min-Max	65.3-190	30.9-171	
n	—	5	8 <sup>a,b</sup>	—

<sup>a</sup> No data was available in the terminal phase for rat c9. Therefore, N was 8 for the parameters AUC<sub>0-∞</sub>, k, T<sub>1/2</sub>, CL/F and V/F.

<sup>b</sup> n = 9 for C<sub>max</sub> and T<sub>max</sub>.

<sup>c</sup> Ratio ((L-dopa with benserazide)/benserazide) was estimated with geometric means.

The absorption rate constant of L-dopa was higher after treatment with L-dopa than after L-dopa/benserazide. L-dopa is a large neutral amino acid (LNAA) and is absorbed via the saturable LNAA-system (3,4). If L-dopa is administered together with benserazide, the metabolism of L-dopa to dopamine in the gut is inhibited. As a consequence higher amounts of L-dopa and 3-OMD, two competing substrates for the carrier (3), are available for transport than after administration of L-dopa alone. This competition determines the flux of each competing substrate across the membrane and may explain why we observed a slower absorption rate after L-dopa/benserazide than after L-dopa.

The between-animal variability was high for the L-dopa parameters C<sub>max</sub> and T<sub>max</sub> after L-dopa and for T<sub>max</sub> and k<sub>a</sub> after L-dopa/benserazide. Bredberg *et al.* (9) made similar observations with regard to T<sub>max</sub> and C<sub>max</sub> after combined oral administration of L-dopa and carbidopa and attributed this to factors influencing gastric emptying. These findings are

in agreement with the marked inter-patient variability in T<sub>max</sub> and C<sub>max</sub> in humans after oral L-dopa administration (29-31).

The terminal log-linear phase of 3-OMD after treatment with L-dopa and L-dopa/benserazide extended over 16-20 h and was thus defined over less than 2 half-lives. Nevertheless, the elimination rate constant of 3-OMD could be estimated well by linear regression. It was similar to the elimination rate constant obtained by compartmental analysis (Table VI) and from the literature (32).

Substantial effort was spent to fit models to the data after L-dopa and after L-dopa/benserazide keeping the 3-OMD clearance and the 3-OMD volume of distribution the same for both treatment groups. However, this resulted in an underestimation of the 3-OMD plasma concentrations after L-dopa/benserazide and in a high estimation error for k<sub>i</sub>. The fit became satisfactory only when allowing for different values for those two parameters in each treatment (the Akaike Information Criteria (33) improved from 3868 to 3790). The fact

**Table IV.** Kinetic Parameters of Ro 04-5127 After Treatment with Benserazide or L-Dopa/Benserazide (Noncompartmental Analysis)

		Treatment		Ratio <sup>a</sup> [95% CI]
		Benserazide	L-Dopa/Benserazide	
AUC <sub>0-∞</sub>	Mean (CV%)	0.309 (42%)	0.321 (19%)	1.10 [0.78; 1.55]
[h · μmol/l]	Min-Max	0.171-0.502	0.249-0.435	
C <sub>max</sub>	Mean (CV%)	0.579 (79%)	0.621 (59%)	1.20 [0.47; 3.03]
[μmol/l]	Min-Max	0.143-1.15	0.184-1.19	
T <sub>max</sub>	Median	0.17	0.10	—
[h]	Min-Max	0.083-0.27	0.083-0.50	
k	Mean (CV%)	0.525 (23%)	0.798 (42%)	1.40 [0.82; 2.41]
[h <sup>-1</sup> ]	Min-Max	0.363-0.642	0.275-1.25	
T <sub>1/2</sub>	Mean (CV%)	1.38 (26%)	1.10 (60%)	0.71 [0.42; 1.22]
[h]	Min-Max	1.08-1.91	0.553-2.52	
n	—	5	9	—

<sup>a</sup> Ratio ((L-dopa with benserazide)/benserazide) was estimated with geometric means.

Table V. Kinetic Parameters Estimated by Compartmental Analysis

Analyte	PK Parameter [Unit]	Estimate	CV% <sup>c</sup>
L-Dopa	$V_{dopa}$ [l]	0.496	9
	$CL_{dopa}$ [l/h] 80 mg/kg L-dopa	0.823	9
3-OMD	$V_{OMD,b}$ [l] 80 mg/kg L-dopa	0.196	13
	$V_{OMD,c}$ [l] 80/20 mg/kg L-dopa/benserazide	0.128	5
	$CL_{OMD,b}$ [l/h] 80 mg/kg L-dopa	0.0120	27
	$CL_{OMD,c}$ [l/h] 80/20 mg/kg L-dopa/benserazide	0.00895	11
Benserazide	$CL_B$ [l/h]	1.67	4
	$V_{1B}$ [l]	0.202	6
	$V_{2B}$ [l]	0.127	13
	$CL_{dB}$ [l/h] <sup>a</sup>	0.0720	9
	$ka_B$ [h <sup>-1</sup> ]	0.940	27
Ro 04-5127	$CL_M$ [l/h]	4.29	11
	$V_{1M}$ [l]	0.0691	11
	$V_{2M}$ [l]	3.20	49
	$CL_{dM}$ [l/h] <sup>a</sup>	1.06	5
	$ka_M$ [h <sup>-1</sup> ]	2.47	17
	$ki$ [ $\mu$ mol/l] <sup>b</sup>	0.00246	42

<sup>a</sup> Intercompartmental clearance.

<sup>b</sup> Inhibition constant.

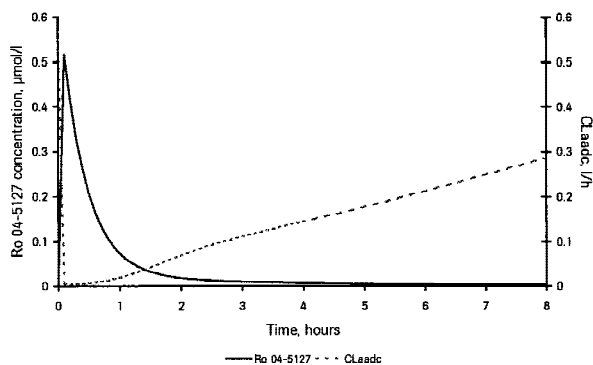
<sup>c</sup> CV% derived from asymptotic standard error of the estimate.

that different values for clearance and volume of distribution had to be introduced for 3-OMD after treatment with L-dopa and with L-dopa/benserazide points to saturability in 3-OMD formation or elimination. In contrast to L-dopa, 3-OMD is a poor substrate for AADC (34). Therefore, the possibility of benserazide influencing the elimination of 3-OMD is judged to be small.

Our study is the first investigation where the kinetics of benserazide and its metabolite Ro 04-5127 could be estimated in rats in some detail due to a newly available quantitative analytical method. Average curves of benserazide and its metabolite Ro 04-5127 look similar. However, this is an artifact of averaging concentrations. When plotting individual benserazide and associated Ro 04-5127 concentration-time profiles together, the metabolite peak was higher and occurred earlier than the benserazide peak. Furthermore, the metabolite Ro 04-5127 declined biphasically. This metabolite-parent compound pattern in the concentration-time profile is typical for drugs where a part of the parent compound is

converted to metabolite during the absorption step (35,36) and where the metabolite's elimination is formation-rate limited. This is the case for benserazide, which is substantially metabolized to Ro 04-5127 in the gut already. Therefore, the terminal half-life of Ro 04-5127 estimated by noncompartmental analysis does not reflect the true elimination half-life of this metabolite.

The benserazide kinetics were described well by the benserazide/Ro 04-5127 model. The final benserazide parameters were in good agreement with values from a previous



<sup>1</sup> The L-dopa clearance by AADC at time zero (no inhibition) was defined as 69% of the total L-dopa clearance. (3)

Fig. 5. Plasma concentration-time profile of Ro 04-5127 and the change of L-dopa clearance by AADC<sup>1</sup> over time after oral administration of 80/20 mg/kg L-dopa/benserazide.

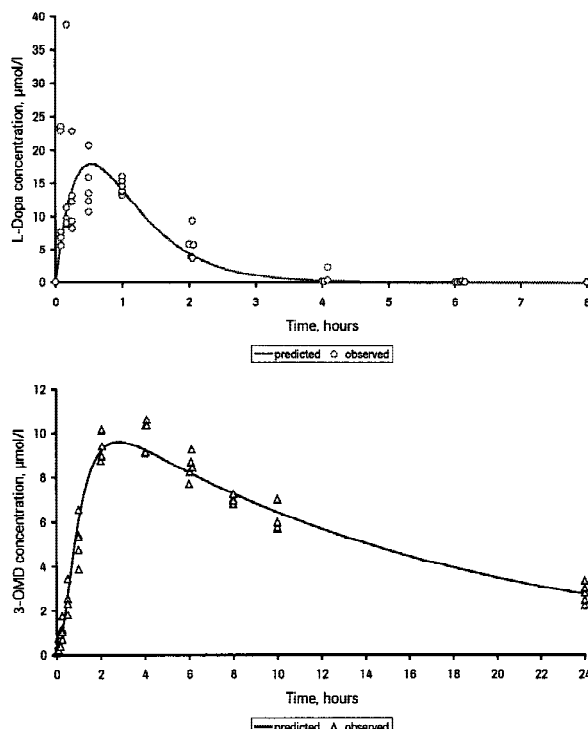


Fig. 6. Predicted and observed L-dopa and 3-OMD plasma concentrations after oral administration of 80 mg/kg L-dopa.



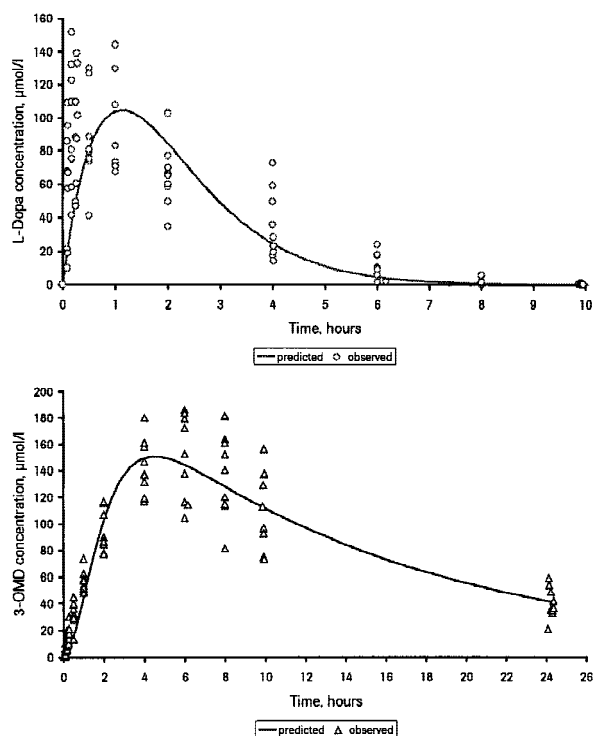


Fig. 7. Predicted and observed L-dopa and 3-OMD plasma concentrations after oral administration of 80/20 mg/kg L-dopa/benserazide.

compartmental analysis. In that analysis, intravenous data of benserazide from two previous studies (20,21) had been fitted simultaneously to a standard 2-compartment model. The kinetic parameters of the present analysis compared to the previous analysis were  $CL_B$ : 1.67 l/h vs. 1.62 l/h,  $V_{1B}$ : 0.202 l vs. 0.186 l,  $V_{2B}$ : 0.127 l vs. 0.115 l, and  $CL_{dB}$ : 0.0720 l/h vs. 0.0685 l/h.

The benserazide parameters estimated by noncompartmental analysis were based on noisy data, where often only few points were available for parameter estimation. Still they were similar to estimates obtained by compartmental analysis where the data were pooled to increase the density of information (compartmental vs. noncompartmental:  $CL/F$ : 76.0 l/h vs. 70.8–95.4 l/h;  $F$  2, 2% assumed for calculation of compartmental values).

The parameters of Ro 04-5127 were based on the four

**Table VI.** Comparison of PK Parameters of L-Dopa and 3-OMD Estimated by Compartmental Analysis (CA) and by Standard Noncompartmental Analysis (NCA)

Analyte	PK parameter [unit]	Estimate (NCA) <sup>b</sup>	Estimate (CA) <sup>a,b</sup>
L-Dopa	V/F [l]	2.22	2.33
	CL/F [l/h]	3.72	3.88
	$k$ [ $h^{-1}$ ] <sup>c</sup>	1.73	1.66
3-OMD	V/F [l]	0.945	0.923
	CL/F [l/h]	0.0563	0.0563
	$k$ [ $h^{-1}$ ] <sup>c</sup>	0.0602	0.0611

<sup>a</sup>  $F = 0.212$  (estimated from  $F_G \cdot F_H$ ).

<sup>b</sup> Calculations done with all significant figures.

<sup>c</sup>  $k$  was estimated by linear regression analysis (NCA) and as a secondary parameter from  $CL/V$  (CA).

assumptions mentioned earlier. Those assumptions did not influence the L-dopa/3-OMD parameters obtained. The benserazide/Ro 04-5127 model parameters adequately described the observations and were fixed when combining them with the L-dopa model. Knowledge on the fraction of benserazide metabolized to Ro 04-5127, resulted from the assumption that the total Ro 04-5127 clearance is not larger than the cardiac output in the rat, which is  $110.4 \pm 15.60$  ml/min (37). Thus the maximum value of  $f_m$  could be estimated from the total Ro 04-5127 clearance which was set to the cardiac output, the area under the plasma concentration-time curve of Ro 04-5127, and the benserazide dose. The  $f_m$  value used in our model, 15%, was then arbitrarily chosen from the possible range 0–30%. Further experiments will be needed to verify these assumptions and confirm the parameters estimated.

Benserazide is chemically a seryl-trihydroxybenzylhydrazine. In neutral, alkaline, or strongly acidic medium it is unstable (12). In the body the seryl-moiety splits off enzymatically liberating trihydroxybenzylhydrazine (Ro 04-5127). In our compartmental model concentrations of Ro 04-5127 and not of benserazide itself were assumed to inhibit AADC based on results by Burkard *et al.* (17). The fact that we obtained a better fit with Ro 04-5127 as inhibitory moiety than with benserazide provides additional evidence for this mechanism of action. The Akaike Information Criteria (33) improved from 3793 to 3790.

In the literature we find mostly 2-compartment models to describe the L-dopa kinetics. It is well known that L-dopa kinetics follow a biexponential decline after intravenous administration in rats, dogs, and humans (1,9–11,27,38). The initial rapid decline of the L-dopa plasma concentration reflects its distribution from plasma to other tissues, primarily muscle (8,39) as well as liver and kidney (40). If L-dopa is administered orally the rapid distribution phase is often masked by the simultaneous absorption of the drug (4,7). This was also seen in the present study where the initial distribution phase was not apparent after oral dosing. Therefore, a 1-compartment model was chosen to describe the L-dopa kinetics of the present study.

For the compartmental analysis the data density of the present study was not sufficient for individual analysis. We decided to pool the data and to fit the model to all individual observations simultaneously (naïve pooled data approach). The disadvantage of pooling is masking of the individual behavior and distortion of the model structure and parameter estimates. However, the profiles of individual animals given the same treatments had similar shapes and this encouraged us to believe that pooling the data to explore model features that could not be defined by any one animal would not seriously affect our conclusions.

There are numerous descriptions of drug-drug PK interactions in the literature. They vary from qualitative vs. quantitative to *in vitro* vs. *in vivo* approaches. A drug-drug PK interaction can be described qualitatively. In this case the objective of the study would be to answer the question of an occurrence of a drug-drug PK interaction with yes or no. However, this qualitative information is often not sufficient. There is frequently the need to quantify the drug-drug PK interaction. One approach to do that is to estimate and compare PK parameters (e.g.  $AUC_{0-\infty}$ ,  $C_{max}$ ) of the investigational drug by noncompartmental analysis after treatment

with and without inhibitor. An alternative approach to quantify the interaction is to formulate a mathematical relationship describing the PK drug-drug interaction taking into account the mechanism of the interaction (e.g. type of inhibition, enzymes involved, site of inhibition). In the present study both approaches were applied. The noncompartmental analysis of drug-drug interaction did not necessitate knowledge about the mechanism of the interaction. Therefore, it was a useful tool for checking on a potential bias a model could introduce and for initial quantification of the changes in  $AUC_{0-\infty}$ ,  $C_{max}$ , and  $CL/F$  caused by the interaction of L-dopa and benserazide. However, the limitation of this approach was that it gave no insight into the sequence and progression of events. Without applying a model the only conclusion from this study was that the decrease in  $CL/F$  led to higher exposure of L-dopa. In contrast, the compartmental model had the advantage of describing the temporal change of inhibition and the recovery of enzyme. Thus a more explicit view could be gained on the cause for higher exposure of L-dopa and 3-OMD. PK parameters such as total L-dopa clearance, bioavailability of L-dopa, and fraction of L-dopa metabolized via COMT were allowed to change over time depending on the inhibitor concentration in plasma. The bioavailability of L-dopa increased from 21% (L-dopa) to more than 87% (L-dopa/benserazide). For some time after administration of benserazide the metabolic pathway via AADC was almost blocked after L-dopa/benserazide administration. The L-dopa clearance via AADC decreased within 5 min from 0.568 l/h to 0.00246 l/h and recovered only slowly over 24 h (Fig. 5). This had an influence on the total L-dopa clearance, which was reduced 69% within the first 5 min and recovered over 24 h. Those changes in bioavailability and total clearance resulted in a higher exposure of L-dopa. Due to the inhibition of the AADC pathway the fraction of L-dopa metabolized by COMT increased from 10% to 31% resulting in higher  $AUC_{0-\infty}$  and  $C_{max}$  of 3-OMD. These temporal changes could not be described by noncompartmental analysis. Therefore, the drug-drug PK interaction described with modelling contained more information about what happened when L-dopa and benserazide were administered together. Another advantage of describing the interaction with a model is that it allows simulations. Exploratory analyses can be performed to predict different scenarios such as multiple doses or change in strength of dose. Modelling is a powerful tool to enhance the comprehension of the complex processes defining a PK drug-drug interaction and thus may also prove useful in drug development. However, the modelling approach needs a lot of information and assumptions on the drug behavior. Depending on the development stage of the drug, this information is not always available. This could be a drawback for applying the modelling approach in early phases of drug development.

In conclusion, our study is the first investigation where the kinetics of benserazide and Ro 04-5127 have been described by a compartmental model. The L-dopa/benserazide model allowed a mechanism-based view of the PK interaction of L-dopa/benserazide and supports the hypothesis that Ro 04-5127 is the primary active metabolite of benserazide.

## REFERENCES

1. G. F. Wooten. Pharmacokinetics of levodopa. In C. D. Marsden and S. Faka (eds.), *Movement Disorders*, Butterworths, 1984 pp. 231-240.
2. Dopamine Hydrochloride. In *Martindale*, The Pharmaceutical Press, London, 1999 pp. 861-862.
3. J. G. Nutt and J. H. Fellman. Pharmacokinetics of levodopa. *Clin. Neuropharmacol.* **7**:35-49 (1984).
4. J. G. Nutt. Pharmacokinetics of levodopa. In W. C. Koller (ed.), *Handbook of Parkinson's Disease*, Marcel Dekker Inc., New York-Basel, pp. 339-354.
5. H. J. Doller, J. D. Connor, D. R. Lock, R. S. Sloviter, B. H. Dvorchik, and E. S. Vesell. Levodopa pharmacokinetics: Alterations after benserazide, a decarboxylase inhibitor. *Drug Metab. Dispos.* **6**:164-168 (1978).
6. P. S. Leppert, M. Cortese, and J. A. Fix. The effects of carbidopa dose and time and route of administration on systemic L-dopa levels in rats. *Pharm. Res.* **5**:587-591 (1988).
7. S. Rose, P. Jenner, and C. D. Marsden. Peripheral pharmacokinetic handling and metabolism of L-dopa in the rat: The effect of route of administration and carbidopa pretreatment. *J. Pharm. Pharmacol.* **43**:325-330 (1991).
8. S. Rose, P. Jenner, and C. D. Marsden. The effect of carbidopa on plasma and muscle levels of L-dopa, dopamine, and their metabolites following L-dopa administration to rats. *Mov. Disord.* **3**:117-125 (1988).
9. E. Bredberg, H. Lennernaes, and L. K. Paalzow. A study of the pharmacokinetics of levodopa in the rat following different routes of administration. *Pharm. Res.* **11**:549-555 (1994).
10. S. Sato, T. Koitabishi, and A. Koshiro. Pharmacokinetic and pharmacodynamic studies of L-dopa in rats. I. Pharmacokinetic analysis of L-dopa in rat plasma and striatum. *Biol. Pharm. Bull.* **17**:1616-1621 (1994).
11. K. Iwamoto, J. Watanabe, M. Yamada, F. Atsumi, and T. Matsushita. Effect of age on gastrointestinal and hepatic first-pass effects of levodopa in rats. *J. Pharm. Pharmacol.* **39**:421-425 (1987).
12. D. E. Schwartz and R. Brandt. Pharmacokinetic and metabolic studies of the decarboxylase inhibitor benserazide in animals and man. *Arzneimittelforschung* **28**:302-307 (1978).
13. M. Schleimer and G. Fischer. Determination of endogenous L-dopa and 3-O-methyldopa together with carbidopa or benserazide and (2,3,4-Trihydroxybenzyl)hydrazine in human plasma using solid phase extraction and HPLC with electrochemical detection. *Data on File*, Hoffmann-La Roche Ltd., Basel, 1996.
14. M. Schleimer and G. Fischer. Determination of benserazide (Ro 04-4602) and (2,3,4-Trihydroxybenzyl)hydrazine (Ro 04-5127) in human, dog and rat plasma using HPLC with electrochemical detection. *Data on File*, Hoffmann-La Roche Ltd., Basel, 1996.
15. M. Gibaldi and D. Perrier. Method of residuals. In *Pharmacokinetics*, Marcel Dekker Inc., New York-Basel, 1982 pp. 433-444.
16. S. Riegelman and P. Collier. The application of statistical moment theory to the evaluation of in vivo dissolution time and absorption time. *J. Pharmacokinetic. Biopharm.* **8**:509-534 (1980).
17. W. Burkard, K. Gey, and A. Pletscher. Inhibition of decarboxylase of aromatic amino acids by 2,3,4-trihydroxybenzylhydrazine and its seryl derivative. *Arch. Biochem. Biophys.* **107**:187-196 (1964).
18. B. Davies and T. Morris. Physiological parameters in laboratory animals and humans [editorial]. *Pharm. Res.* **10**:1093-1095 (1993).
19. P. T. Mearrick, G. G. Graham, and D. N. Wade. The role of the liver in the clearance of L-dopa from plasma. *J. Pharmacokinetic. Biopharm.* **3**:13-23 (1975).
20. M. Schmitt, M. Schleimer, and G. Fischer. Effect of tolcapone on benserazide (Ro 04-4602) plasma levels in rats. *Data on File*, F. Hoffmann-La Roche Ltd., Basel, 1996.
21. M. Schmitt, M. Schleimer, G. Fischer, M. S. Gruyer, and P. Schrag. Benserazide exposure in rats and dogs after oral administration. *Data on File*, F. Hoffmann-La Roche Ltd., Basel, 1997.
22. L. F. Lacey, O. N. Keene, J. F. Pritchard, and A. Bye. Common noncompartmental pharmacokinetic variables: Are they normally or log-normally distributed? *J. Biopharm. Stat.* **7**:171-178 (1997).
23. L. Landsberg, M. B. Berardino, and P. Silva. Metabolism of 3-H-L-dopa by the rat gut in vivo-evidence for glucuronide conjugation. *Biochem. Pharmacol.* **24**:1167-1174 (1975).
24. L. Rivera Calimlim, C. A. Dujoyne, J. P. Morgan, L. Lasagna,

- and J. R. Bianchine. Absorption and metabolism of L-dopa by the human stomach. *Eur. J. Clin. Invest.* **1**:313-320 (1971).
25. K. Sasahara, T. Nitanaï, T. Habara, T. Kojima, Y. Kawahara, T. Morioka, and E. Nakajima. Dosage form design for improvement of bioavailability of levodopa IV: Possible causes of low bioavailability of oral levodopa in dogs. *J. Pharm. Sci.* **70**:730-733 (1981).
  26. G. M. Tyce. Metabolism of 3,4-dihydroxyphenylalanine by isolated perfused rat liver. *Biochem. Pharmacol.* **20**:3447-3462 (1971).
  27. S. Cotler, A. Holazo, H. G. Boxenbaum, and S. A. Kaplan. Influence of route of administration on physiological availability of levodopa in dogs. *J. Pharm. Sci.* **65**:822-827 (1976).
  28. G. M. Tyce and C. A. Owen. Administration of L-3,4-dihydroxyphenylalanine to rats after complete hepatectomy-II. Excretion of metabolites. *Biochem. Pharmacol.* **28**:3279-3284 (1979).
  29. H. Hinterberger and C. J. Andrews. Catecholamine metabolism during oral administration of levodopa. *Arch. Neurol.* **26**:245-252 (1972).
  30. W. B. Abrams, C. B. Coutinho, A. S. Leon, and H. E. Spiegel. Absorption and metabolism of levodopa. *JAMA* **218**:1912-1914 (1971).
  31. D. N. Wade, P. T. Mearrick, D. J. Birkett, and J. Morris. Variability of L-dopa absorption in man. *Aust. NZ J. Med.* **4**:138-143 (1974).
  32. G. Bartholini, I. Kuruma, and A. Pletscher. Distribution and metabolism of L-3-O-methyldopa in rats. *Br. J. Pharmacol.* **40**:461-467 (1970).
  33. J. Gabrielsson and D. Weiner. Discrimination between rival models. In *Pharmacokinetic and Pharmacodynamic Data Analysis: Concepts and Applications*, Swedish Pharmaceutical Press, Stockholm, Sweden, 1997 pp. 307-309.
  34. R. Ferrini and A. Glässer. *In vitro* decarboxylation of new phenylalanine derivatives. *Biochem. Pharmacol.* **13**:798 (1964).
  35. M. Rowland and T. N. Tozer. Metabolite kinetics. In *Clinical Pharmacokinetics: Concepts and Applications*, Lea & Febiger, Philadelphia-London, 1989 pp. 347-375.
  36. T. Walle, T. C. Fagan, E. C. Conradi, U. K. Walle, and T. E. Gaffney. Presystemic and systemic glucuronidation of propranolol. *Clin. Pharmacol. Ther.* **26**:167-172 (1979).
  37. R. P. Brown, M. D. Delp, S. L. Lindstedt, L. R. Rhomberg, and R. P. Beliles. Physiological parameter values for physiologically based pharmacokinetic models. *Toxicol. Ind. Health* **13**:407-484 (1997).
  38. K. Sasahara, T. Nitanaï, T. Habara, T. Morioka, and E. Nakajima. Dosage form design for improvement of bioavailability of levodopa II: bioavailability of marketed levodopa preparations in dogs and parkinsonian patients. *J. Pharm. Sci.* **69**:261-265 (1980).
  39. J. A. Romero, L. D. Lytle, L. A. Ordonez, and R. J. Wurtman. Effects of L-dopa administration of the concentrations of dopa, dopamine and norepinephrine in various rat tissues. *J. Pharmacol. Exp. Ther.* **184**:67-72 (1973).
  40. G. A. Lyles. Effects of L-DOPA administration upon monoamine oxidase activity in rat tissues. *Life Sci.* **22**:603-609 (1978).